

Dielectric, ferroelectric, and pyroelectric characterization of Mn-doped $0.74\text{Pb}(\text{Mg}_{1/3}\text{Nb}_{2/3})\text{O}_3-0.26\text{PbTiO}_3$ crystals for infrared detection applications

Linhua Liu,^{1,2,a)} Xiaobing Li,^{1,2} Xiao Wu,^{1,2} Yaojin Wang,^{1,2} Wenning Di,¹ Di Lin,¹ Xiangyong Zhao,¹ Haosu Luo,¹ and Norbert Neumann³

¹Shanghai Institute of Ceramics, Chinese Academy of Sciences, 215 Chengbei Road, Jiading, Shanghai 201800, People's Republic of China

²Graduate University of Chinese Academy of Sciences, Beijing 100049, People's Republic of China

³InfraTec GmbH Infrarotmesstechnik und Sensorik, Dresden 01217, Germany

(Received 2 October 2009; accepted 21 October 2009; published online 11 November 2009)

We investigated the dielectric, ferroelectric, and pyroelectric properties of Mn-doped $0.74\text{Pb}(\text{Mg}_{1/3}\text{Nb}_{2/3})\text{O}_3-0.26\text{PbTiO}_3$ crystals. Compared with pure PMN-0.26PT, Mn substitutions resulted in reduced dielectric loss and enhanced coercive field. Furthermore, the pyroelectric coefficient and detectivity figures of merits were enhanced to $17.2 \times 10^{-4} \text{ C/m}^2 \text{ K}$ and $40.2 \times 10^{-5} \text{ Pa}^{-1/2}$, respectively, which were the highest values so far reported among intrinsic pyroelectric materials with rhombohedral-tetragonal phase transition temperature greater than 90°C . The specific detectivity of infrared detector based on Mn-doped crystals was $1.07 \times 10^9 \text{ cm Hz}^{1/2} \text{ W}^{-1}$, and approximately doubles that of commercial LiTaO_3 crystals-based, which makes them promising candidates for infrared detectors applications. © 2009 American Institute of Physics. [doi:10.1063/1.3263139]

Much attention has been focused on high performance pyroelectric materials and their applications. Infrared detectors made by pyroelectric materials have the advantages of their wide wavelength response, no requirement for cooling, high temperature stability, high sensitivity, and low cost. Consequently, they are widely used in consumer products such as fire alarms and intruder detectors, in instrumentation such as gas analysis and laser beam characterization, and in military/paramilitary applications such as thermal imaging, particularly where untended operation is required.^{1,2}

It is general to select pyroelectric materials for practical device applications upon the figures of merits (FOMs),¹ where current responsivity $F_i = p/C_v$, voltage responsivity $F_v = p/(C_v \epsilon_0 \epsilon_r)$, and detectivity $F_d = p/[C_v(\epsilon_0 \epsilon_r \tan \delta)^{1/2}]$ should be considered upon the working mode. p , C_v , ϵ_0 , ϵ_r , and $\tan \delta$ are the pyroelectric coefficient, volume specific heat, permittivity of free space, dielectric constant, and dielectric loss, respectively. $(1-x)\text{Pb}(\text{Mg}_{1/3}\text{Nb}_{2/3})\text{O}_3-x\text{PbTiO}_3$ (PMN- x PT, PMN-PT) and $(1-x)\text{Pb}(\text{Zn}_{1/3}\text{Nb}_{2/3})\text{O}_3-x\text{PbTiO}_3$ (PZN- x PT, PZN-PT) single crystals have been reported to be the promising pyroelectric materials, especially $[111]$ oriented rhombohedral PMN- x PT crystals with $0.26 \leq x \leq 0.28$.^{3,4} To reduce dielectric loss and depress dielectric noises are crucial issues for the relaxor-based ferroelectrics when they are used as pyroelectric materials, because dielectric loss is around 0.003 for PMN-PT single crystals, however it is about 0.0005 for commercial LiTaO_3 single crystals.

Recently, the effect of additive on PZN-PT and PMN-PT system has been investigated, especially as iron (Fe) and manganese (Mn) substitutions.^{5–11} It was found that the Fe substitutions do not significantly affect the properties of PZN-PT, PMN-PT, while Mn substitutions are found to bring

hard characteristics to enhance coercive field (E_C) and reduce dielectric loss. However, the majority researches on Mn substitutions focused on improving piezoelectric properties, as in PMN-0.29PT single crystals,¹¹ while the effect of Mn substitutions on PMN-0.26PT crystals with superior pyroelectric properties has never been investigated. In the present letter, we reported our results on Mn-doped effects for PMN-0.26PT crystals to improve the pyroelectric performances for new generation infrared detection applications.

Single crystals of 1 mol % Mn-doped PMN-0.26PT (Mn-doped PMN-0.26PT) were grown directly from melt by the modified Bridgman technique.¹² The raw powders of MnO_2 , PbO , MgO , Nb_2O_5 , and TiO_2 with purity more than 99.99% are used as the starting materials. B-site precursor synthesis method is used to prevent formation of the pyrochlore phase during crystals growth.¹³ Usually high quality single crystals with a large size of about $\Phi 50 \times 80 \text{ mm}^3$ could be obtained. X-ray diffraction analysis was employed to confirm the presence of a pure perovskite phase. The as-grown crystal was cut as (111) wafers because high values of pyroelectric coefficients appear along the spontaneous polarization direction $[111]$.¹⁴ For the electrical characterization, the crystal was cut into specimens with dimensions of $4 \times 4 \times 0.6 \text{ mm}^3$, and polished by Al_2O_3 powder. Silver paste was painted on the main surface of crystal and sintered at 700°C for 30 min. Then, the samples were poled perpendicular to main surface under an electric field of 10 kV/cm for 15 min at 120°C and then slowly cooled to room temperature in silicone oil with a half electric field.

Figures 1(a) and 1(b) show the dielectric constant and dielectric loss as a function of temperature and frequency for $[111]$ oriented Mn-doped and pure PMN-0.26PT crystals measured by a HP4194A impedance analyzer. The permittivity ϵ_r has a peak at the Curie temperature (T_C), 120°C and then a shoulder at the ferroelectric rhombohedral to tetrago-

^{a)}Electronic mail: mserllh@163.com.

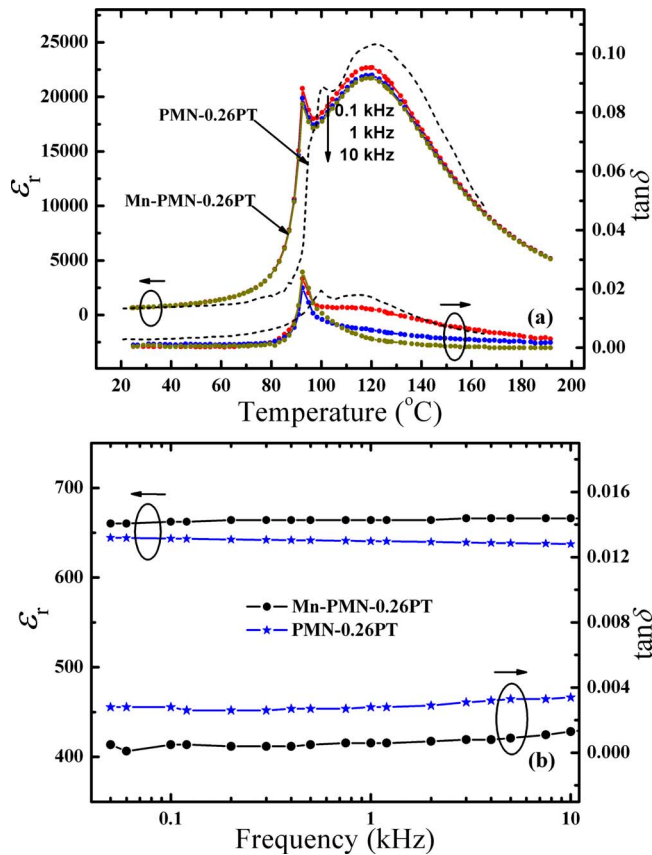


FIG. 1. (Color online) Dielectric characteristics of poled [111] oriented Mn-doped PMN-0.26PT and pure PMN-0.26PT crystals. (a) Temperature dependence at 0.1, 1, and 10 kHz and (b) frequency dependence at 25 °C. The data of pure crystals were taken from Ref. 3.

nal phase transition temperature (T_{RT}), 95 °C during the cooling process. Both the T_C and T_{RT} of Mn-doped PMN-0.26PT crystals are a few lower than pure PMN-0.26PT, which was also observed in Mn-doped single crystals of PZN and PZNT.^{5,6} At 25 °C, the dielectric constants increase after doped Mn^{4+} ions, while the dielectric loss of doped crystals is lower than that of pure ones. The value of $\tan \delta$ of doped crystals is 0.0005 at 50 Hz, and increases to 0.0013 at 10 000 Hz, which is much smaller than about 0.003 of pure crystals. It also can be seen that there are weak frequency dispersion for dielectric constant and loss.

The P - E hysteresis loops of Mn-doped and pure PMN-0.26PT crystals, tested using a Sawyer–Tower circuit at 25 °C and 10 Hz, are shown in Fig. 2. The remnant polarization (P_r) of Mn-doped PMN-0.26PT crystals is 42 $\mu C/cm^2$, and E_C is 4.5 kV/cm, showing a positive offset of 0.5 kV/cm contributed by oxygen vacancy defect-dipoles.¹⁵ The P_r and E_C of pure PMN-0.26PT are 35 $\mu C/cm^2$ and 2.6 kV/cm, respectively. Therefore, the Mn-doped PMN-0.26PT crystals are expected to be more stable when an inverse electric field is applied in the poling direction. Higher values of P_r and E_C with Mn doping are due to the polarization pinning by dipole defects, which makes the crystals become “hard” and tend to form macrodomain configuration.

The pyroelectric coefficient (p) was measured by a dynamic technique¹⁶ using sinusoidal temperature change with amplitude of 0.25 °C at a frequency of 45 mHz. Figure 3 shows the temperature dependence of pyroelectric

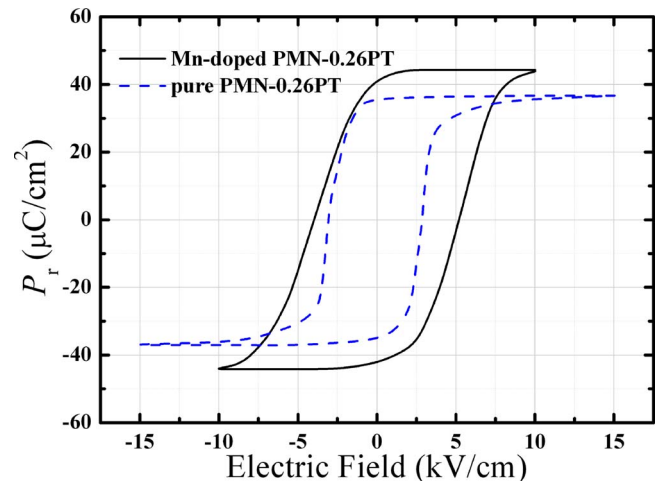


FIG. 2. (Color online) P - E hysteresis loops of [111] oriented Mn-doped PMN-0.26PT crystals compared with pure PMN-0.26PT at 25 °C and 10 Hz.

coefficient for Mn-doped PMN-0.26PT single crystals from 20 °C to 60 °C. The value of p reaches as high as 17.2×10^{-4} C/m² K at 25 °C, larger than that of PZT (3.3×10^{-4} C/m² K) and LiTaO₃ (2.3×10^{-4} C/m² K).¹⁷ With increasing temperature, p is almost linearly up to 25.9×10^{-4} C/m² K at 60 °C. Table I summarizes the pyroelectric and related properties of Mn-doped and pure PMN-0.26PT crystals compared with other typical pyroelectric materials at 25 °C. The detectivity FOM of $F_d = 40.2 \times 10^{-5}$ Pa^{-1/2} is the highest value so far reported among intrinsic pyroelectric materials with T_{RT} greater than 90 °C.

The single element pyroelectric detector was fabricated based on Mn-doped PMN-0.26PT crystals. The pyroelectric chip was $\Phi 2$ mm \times 33 μ m in size electroded with Ni/Cr, while the outface was coated with extra gold-black layer in consideration of thermal absorption. The detector was irradiated by chopped infrared radiation from a blackbody furnace at 500 K with a frequency of 12.5 Hz. The results of voltage responsivity (R_v) and specific detectivity (D^*) are 14 540 V/W and 1.07×10^9 cm Hz^{1/2} W⁻¹, respectively. The performance has already met the requirement of the practical device, and the prototype still need to reduce the thickness to improve its performances.

In summary, the dielectric, ferroelectric, and pyroelectric properties of 1 mol % Mn-doped PMN-0.26PT crystals were investigated. The dielectric loss of Mn-doped PMN-0.26PT crystals was declined to 0.0005, which is much smaller than

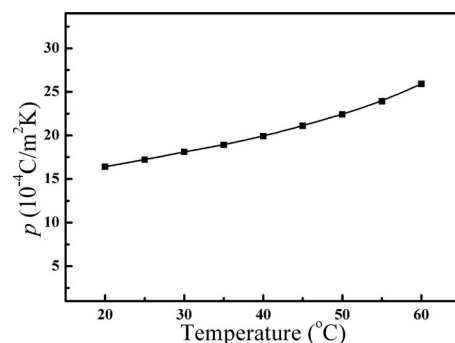


FIG. 3. Temperature dependence of pyroelectric coefficient for Mn-doped PMN-0.26PT single crystals from 20 °C to 60 °C.

TABLE I. Pyroelectric properties of [111] oriented Mn-doped PMN-0.26PT crystals and other typical pyroelectric materials at 25 °C.

Materials	T_C (°C)	T_{RT} (°C)	C_V (10^6 J/m ³ K)	p (10^{-4} C/m ² K)	ϵ_r (@100 Hz)	$\tan \delta$ (@100 Hz)	F_i^a (10^{-10} m/V)	F_v^b (m ² /C)	F_d^c (10^{-5} Pa ^{-1/2})	Reference
PMN-0.26PT	122	100	2.5	15.3	643	0.0028	6.1	0.11	15.3	3
Mn-doped PMN-0.26PT	120	95	2.5	17.2	660	0.0005	6.88	0.12	40.2	This work
PZT	340	/	2.5	3.3	714	0.018	1.22	0.02	1.2	17
LiTaO ₃	620	/	3.2	2.3	47	0.0005	0.72	0.17	15.7	17

^aCalculated from the equation $F_i = p/C_V$.^bCalculated from the equation $F_v = p/(C_V \epsilon_0 \epsilon_r)$.^cCalculated from the equation $F_d = p/[C_V(\epsilon_0 \epsilon_r \tan \delta)^{1/2}]$.

that of pure ones. The E_C of Mn-doped PMN-0.26PT crystal was 4.5 kV/cm, nearly 75% larger than that of pure one. Due to the domain wall pinning by dipole defects, the pyroelectric performance is enhanced a lot, $p = 17.2 \times 10^{-4}$ C/m² K and $F_d = 40.2 \times 10^{-5}$ Pa^{-1/2}, which are the highest values so far reported among intrinsic pyroelectric materials with T_{RT} greater than 90 °C. The specific detectivity, crucial parameter of infrared detectors, based on Mn-doped PMN-0.26PT crystals was 1.07×10^9 cm Hz^{1/2} W⁻¹, which approximately doubles that of LiTaO₃ crystals-based infrared detectors commercialized.

This work was financially supported by the Ministry of Science and Technology of China through 863 Program (Grant No. 2008AA03Z410) and 973 Program (Grant No. 2009CB623305), the Natural Science Foundation of China (Grant Nos. 60837003, 50777065, and 50602047), Shanghai Municipal Government (Grant No. 08JC1420500), the Innovation Fund of Shanghai Institute of Ceramics (Grant No. O99ZC4140G), and the Fund of National Engineering Research Center for Optoelectronic Crystalline Materials (Grant No. 2005DC105003-2007K05).

- ¹R. Whatmore, *Rep. Prog. Phys.* **49**, 1335 (1986).
- ²A. Rogalski, *Prog. Quantum Electron.* **27**, 59 (2003).
- ³Y. Tang and H. Luo, *J. Phys. D* **42**, 075406 (2009).
- ⁴B. J. Fang, J. H. Li, H. Q. Xu, and H. S. Luo, *Appl. Phys. Lett.* **91**, 062902 (2007).
- ⁵K. Harada and Y. Yamashita, *Ferroelectrics* **217**, 273 (1998).
- ⁶S. Priya, K. Uchino, and D. Viehland, *Jpn. J. Appl. Phys., Part 2* **40**, L1044 (2001).
- ⁷S. Priya, K. Uchino, and D. Viehland, *Appl. Phys. Lett.* **81**, 2430 (2002).
- ⁸X. M. Wan, X. Y. Zhao, H. S. Luo, H. L. W. Chan, and C. L. Choy, *J. Am. Ceram. Soc.* **88**, 3063 (2005).
- ⁹S. Priya and K. Uchino, *J. Appl. Phys.* **91**, 4515 (2002).
- ¹⁰Y. Tang, L. Luo, Y. Jia, H. Luo, X. Zhao, H. Xu, J. Sun, X. Meng, J. Zhu, and M. Es-Souni, *Appl. Phys. Lett.* **89**, 162906 (2006).
- ¹¹L. H. Luo, D. Zhou, Y. X. Tang, Y. M. Jia, H. Q. Xu, and H. S. Luo, *Appl. Phys. Lett.* **90**, 102907 (2007).
- ¹²H. Luo, G. Xu, H. Xu, P. Wang, and Z. Yin, *Jpn. J. Appl. Phys., Part 1* **39**, 5581 (2000).
- ¹³M. Orita, H. Satoh, K. Aizawa, and K. Ametani, *Jpn. J. Appl. Phys., Part 1* **31**, 3261 (1992).
- ¹⁴M. Davis, D. Damjanovic, and N. Setter, *J. Appl. Phys.* **96**, 2811 (2004).
- ¹⁵G. E. Pike, W. L. Warren, D. Dimos, B. A. Tuttle, R. Ramesh, J. Lee, V. G. Keramidas, and J. T. Evans, *Appl. Phys. Lett.* **66**, 484 (1995).
- ¹⁶L. Garn and E. Sharp, *J. Appl. Phys.* **53**, 8974 (1982).
- ¹⁷B. M. Kulwicki, A. Amin, H. R. Beratan, and C. M. Hanson, *Proc. 8th Int. Symp. on Applications of Ferroelectrics*, Greenville SC, 30 August–2 September 1992 (IEEE, New York, 1992), p. 1.